

ONSET OF SLUGGING OF STAGNANT LIQUID AT A V-SHAPED ELBOW IN A PIPE-LINE: EXPERIMENT AND NUMERICAL SIMULATION

Motoki IRIKURA^{1*}, Munenori MAEKAWA^{2*}, Shigeo HOSOKAWA^{1*} and Akio TOMIYAMA^{1*}

¹ Graduate School of Engineering, Kobe University, 1-1 Rokkodai, Nada-ku, Kobe-shi, Hyogo, 657-8501, JAPAN

² Chiyoda Advanced Solutions Co., Technowave 100 Bldg., 1-25, Shin-Urashima-cho 1-chome, Kanagawa-ku, Yokohama 221-0031, JAPAN

*Corresponding author, E-mail address: motoki.irikura@chas.chiyoda.co.jp

ABSTRACT

Slugging of a stagnant liquid at a V-shaped elbow in a hilly-terrain pipeline is experimentally and numerically investigated. Flow patterns and the onset of slugging are observed using a high-speed camera. The flow in the pipeline is classified into seven flow regimes, i.e. static puddle, wavy puddle, periodic slug flow, periodic semi-slug flow, aperiodic semi-slug flow, film flow and pebble flow. The onset of slugging is well correlated in terms of the Wallis parameter, which has been utilized for modelling flooding phenomena in a pipe. This means that the slugging at the V-shaped elbow is similar to the flooding caused by interfacial shear stress. An empirical correlation based on a modified Wallis parameter is proposed to represent the effects of inclination angle, pipe diameter and fluid properties on the onset of slugging. Numerical simulation is carried out to predict the onset of slugging using a three-dimensional two-fluid model in commercial software CFX 13. The free surface treatment for the interfacial area density is employed to describe the interaction between the phases. Comparison with experimental data shows that this numerical model is able to simulate slug development from static or wavy puddle. The onset of slugging is also predictable with reasonable accuracy.

NOMENCLATURE

B_o Bond number
D inner diameter of pipe
g acceleration of gravity
h_G distance between interface and upper surface of pipe
J volumetric flux
*J** Wallis parameter
Q_L volume of stagnant liquid
Q_{Lmax} maximum volume of stagnant liquid at a V-section
V velocity
V velocity magnitude
P pressure
ΔP pressure drop at a V-section
F force
A area density

μ viscosity
ν kinematic viscosity
θ inclination angle
ρ density
σ surface tension

Subscript

G gas phase
L liquid phase
k phases
i gas-liquid interface

INTRODUCTION

An oil and gas transport pipeline along a hilly-terrain consists of various pipe elements such as horizontal pipes, vertical pipes, inclined ascending and descending pipes. In such a hilly-terrain pipeline, there are V-shaped elbows between descending and ascending pipes. Increase in flow resistance at start-up and shut-down or pressure fluctuation at low load operation sometimes occurs due to slugging of a stagnant liquid at a V-shaped elbow. For the piping design or the execution of appropriate operation procedure, it is important to predict such slugging phenomena.

Two-phase flow in the horizontal, vertical and inclined straight pipes received much attention so far, and the correlations for the onset of slugging in the straight pipe have been proposed (Kordyban and Ranov, 1970; Wallis and Dobson, 1973; Mishima and Ishii, 1980). With respect to a hilly-terrain pipeline including V-shaped elbows, experimental data for slug velocity, slug length, etc. have been reported (Mishima and Ishii, 1993; Hosokawa and Tomiyama, 2003), and some models for the slug growth and decay along the pipe have been proposed (Zheng, Brill and Shoham, 1993). Numerical calculations for the evolution of slug flow in horizontal pipes have been also performed by Masella et al. (1998), Issa et al. (2003) and Bonizzi et al. (2003). However, our knowledge on the slug initiation is still rudimentary. In particular, there are few studies on slugging at the V-shaped elbow (Fitremann, 1975) in spite of its practical importance.

This study focuses on the slugging of a stagnant liquid at the V-shaped portion between descending and ascending pipes. Flow regimes are observed using a high-speed video camera for various gas volumetric fluxes and volumes of the stagnant liquid. The onset of slugging due to the gas flow is investigated by measuring the critical gas volumetric flux at the slug initiation. An empirical correlation based on a modified Wallis parameter is proposed to represent the effects of inclination angle, pipe diameter and fluid properties on the onset of slugging. Three-dimensional numerical simulation is also carried out

using a two-fluid model to examine the feasibility of numerical prediction of slug initiation.

EXPERIMENT

A schematic of the experimental setup is shown in Fig. 1. It consists of the gas supply section and the test section shown in Fig. 2. Air was used for the gas phase, and water or glycerol-water solution was used for the stagnant liquid. The air from the oil-free-compressor (Hitachi, 7.50U-7V6) enters the test section through the critical nozzle. The relation between the air flow rate and the pressure at the upstream of the critical nozzle were measured by a dry gas meter (Shinagawa Seiki) in advance. The test section made of transparent acrylic resin consists of the descending pipe, ascending pipe and V-shaped elbow as shown in Fig. 2. The inclination angles of the descending and ascending pipes are the same. Pipe diameters $D = 20, 30$ and 40 mm, and pipe inclination angles $\theta = 3^\circ, 5^\circ$ and 7° were tested. A rectifier is installed in the mixing section. The length of the descending pipe is more than $100D$ to establish a fully developed gas flow before the V-section. The gas velocity profile was measured by a hot-wire flow meter (KANOMAX) to confirm that the gas flow field was fully developed in the descending pipe. The length of the ascending pipe is more than 2.5 m to prevent the liquid from flowing out of the outlet. Filtered tap water and two kinds of glycerol-water solution (20% and 40%) were used for the stagnant liquid. Physical properties of the solutions are listed in Table 1.

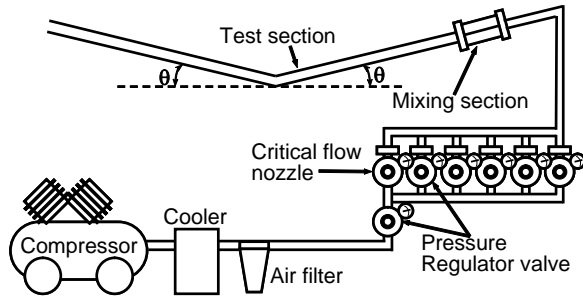


Figure 1: Experimental setup

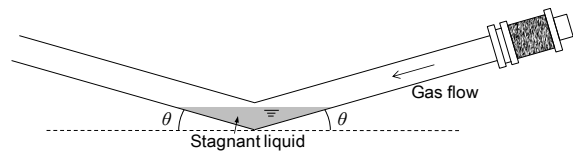


Figure 2: Schematic of test section

Concentration (%)	Density ρ_L (kg/m ³)	Surface tension σ ($\times 10^{-3}$ N/m)	Viscosity μ_L ($\times 10^{-3}$ Pa s)
20	1039	62.9	1.95
40	1081	61.5	5.20

Table 1: Physical properties of glycerol-water solution

The experiment was performed at room temperature. The gas volumetric flux J_G was ranged from 0 to 8 m/s to investigate effects of J_G on flow patterns. The flow patterns were recorded by a high-speed camera (Photron Fast cam rabbit3, shutter speed 1/400 s, frame-rate 400

frame/s). The volume of stagnant liquid Q_L was ranged from 0 ml to the amount enough to fill the pipe cross-section. The liquid was introduced into the V-shaped elbow by a long Teflon tube to avoid wetting the pipe inner surface except the V-section. After accumulating a certain amount of liquid at the V-shaped elbow, the gas volumetric flux J_G was slowly increased to a prescribed value in order to prevent an abrupt increase of J_G from affecting the slug initiation. Then, J_G at the onset of slugging was recorded as a critical gas volumetric flux. The liquid level just before the slugging was measured by a two-wire electrode probe at the center of the elbow to evaluate the gas velocity V_G .

NUMERICAL METHOD

Numerical simulation was performed to predict the onset of slugging using a three-dimensional two-fluid model in the commercial software CFX 13 (ANSYS, 2010). The two-fluid model is based on ensemble-averaged mass and momentum equations for the gas and liquid phases. The incompressible mass and momentum conservation equations are given by

$$\frac{\partial \alpha_k}{\partial t} + \nabla \cdot \alpha_k \mathbf{V}_k = 0 \quad (1)$$

$$\frac{\partial \alpha_k \mathbf{V}_k}{\partial t} + \nabla \cdot \alpha_k \mathbf{V}_k \mathbf{V}_k = -\frac{\alpha_k}{\rho_k} \nabla P + \nabla \cdot \alpha_k \nu_k (\nabla \mathbf{V}_k + (\nabla \mathbf{V}_k)^T) \pm \frac{\mathbf{F}_i}{\rho_k} + \alpha_k \mathbf{g} \quad (2)$$

where the subscript k denotes the gas or liquid phases, ρ is the density, α the phase fraction, \mathbf{V} the velocity, P the pressure, ν the kinematic viscosity and \mathbf{g} the acceleration of gravity. The \mathbf{F}_i in the right hand side of Eq.(2) is the interfacial force, which is expressed in terms of the drag coefficient C_D and the interfacial area density A_i as follows:

$$\mathbf{F}_i = \frac{1}{8} C_D A_i \rho_{GL} |\mathbf{V}_G - \mathbf{V}_L| (\mathbf{V}_G - \mathbf{V}_L) \quad (3)$$

where $(\mathbf{V}_G - \mathbf{V}_L)$ is the relative velocity and ρ_{GL} the mixture density ($= 0.5\rho_G + 0.5\rho_L$). The drag coefficient is set at $C_D = 3.5$. The free surface treatment in CFX13 utilizes the following expression for the interfacial area density A_i .

$$A_i = |\nabla \alpha_L| \quad (4)$$

where α_L is the liquid volume fraction. Equation (4) has been used in interface tracking methods and might be appropriate for simulating separated flows such as stratified flow and wavy flow.

Since J_G at the onset of slugging obtained by the experiment was relatively small and the gas flow was almost within the range of laminar flow or transition region, the present simulation did not account for turbulence. The effect of turbulence on the onset of slugging will be discussed in future work. The simulation domain is illustrated in Fig. 3. Simulating the complete test facility is not practical only for the prediction of slug initiation. To perform a transient simulation within an acceptable CPU time, only the region including the V-shaped elbow was modelled. The lengths of straight pipes in the upstream and the downstream of the V-section are $50D$. The computational grid shown in Fig. 4 was created by ICEM-CFD 13 (ANSYS, 2010) and it consists of 55,000 hexahedral elements. Mesh dependency was also checked with 15,000 and 311,000 elements, by which we confirmed that the mesh size had minor effects on the onset of slugging. In accordance with the experiments, J_G was slowly increased to remove the effect of acceleration

due to a sudden rise of J_G . The J_G at the onset of slugging was investigated in the simulation.

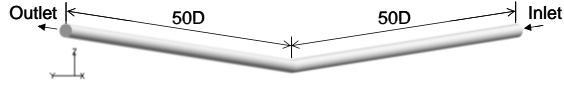


Figure 3: Simulation domain

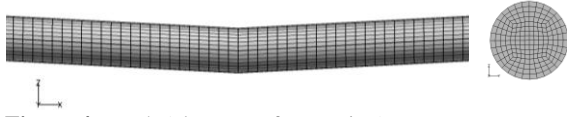


Figure 4: Mesh (close-up of V-section)

RESULTS AND DISCUSSIONS

Flow patterns

Based on the observation in the experiments, the flow regimes were classified into seven regimes, i.e. static puddle, wavy puddle, periodic slug flow, periodic semi-slug flow, aperiodic semi-slug flow, film flow and pebble flow as shown in Fig. 5. Figure 6 shows the flow pattern map for $D = 20$ mm and $\theta = 3^\circ$.

At low J_G , the liquid remains as static puddle (Fig. 5 (a)). In this regime, the gas-liquid interface shows a hump shape due to the Venturi effect, i.e., the suction of the interface is caused by the low pressure due to the high velocity of gas passing through the narrow area at the center of the V-section. This static puddle regime is also kept at higher J_G when Q_L is low enough (Fig. 6). Increase in J_G causes the transition from static to wavy puddle (Fig. 5 (b)) in which ripples are generated at the liquid surface. This regime was observed in a wider range of J_G with lower Q_L . Further increase in J_G induces the excitation of waves, and a liquid slug is formed when the wave grows up to the top of the pipe. The J_G at this onset of the liquid slug is defined as the critical gas volumetric flux. After the slugging, the pressure rise caused by the blockage of the gas flow blows the liquid slug to the uphill of the pipe and then the liquid slug collapses and returns to the V-section due to the gravity to form another slug. This sequence repeats after the onset of slugging. The formation and collapse of liquid slug periodically repeats at low J_G . This flow regime is referred to as periodic slug flow (Fig. 5 (c)). At higher J_G , periodic semi-slug flow (Fig. 5 (d)) is formed, in which the liquid slug does not fill the entire cross-section of the pipe. Further increase in J_G deteriorates the periodicity of slugging, causing aperiodic semi-slug flow (Fig. 5 (e)). Then, the liquid continuously rises up the ascending pipe without returning to the V-section when the interfacial drag force becomes larger than the gravity force. This regime is film flow (Fig. 5 (g)). At low Q_L and small θ , liquid film breaks up to form pebbles flowing up. This is pebble flow (Fig. 5 (f)). No significant change in flow regime map was found for other D and θ within the range of the present experimental conditions, though the pebble flow was observed only in the case of small inclination angle ($\theta = 3^\circ$). The above observation confirmed that the onset of slugging corresponds approximately to the transition from the static or wavy puddle directly changes to the periodic semi-slug

flow when Q_L is low. In the periodic and aperiodic semi-slug flow, liquid does not fill up the pipe cross-section, and the pressure fluctuation is smaller than that of the periodic slug flow. Thus, in what follows, the onset of slugging corresponding to the transition from the static or wavy puddle to the periodic slug flow is investigated due to its importance in practical engineering.

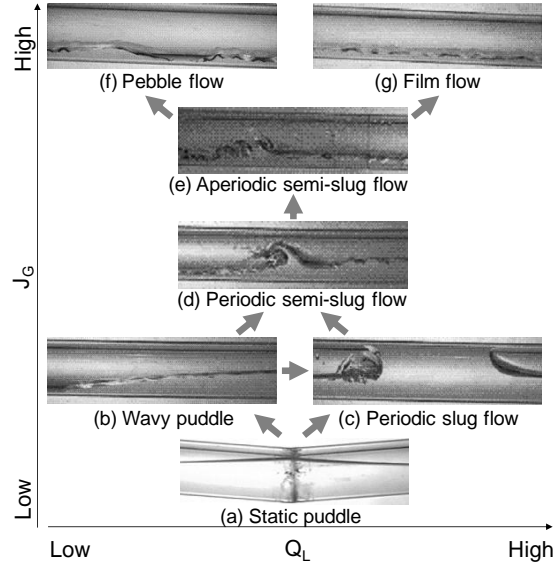


Figure 5: Flow patterns and flow pattern transitions in the V-section and ascending pipe

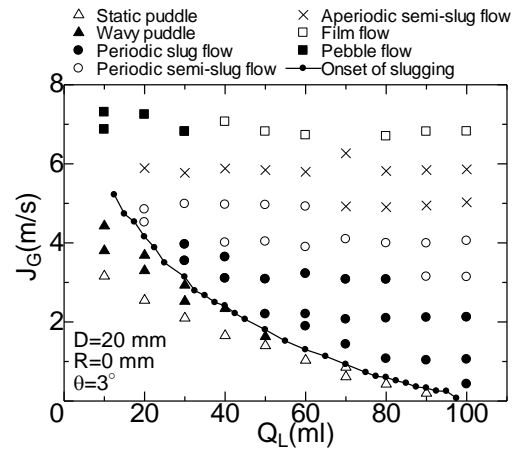


Figure 6: Flow pattern map ($D = 20$ mm, $\theta = 3^\circ$)

Onset of slugging

For the evaluation of the onset of slugging in horizontal pipe, the following criteria was proposed by Mishima and Ishii (1980).

$$V_G - V_L \geq 0.487 \sqrt{\frac{\rho_L g h_G}{\rho_G}} \quad (5)$$

where h_G is the height of the gas flow channel (the distance from the gas-liquid interface to the top wall of the pipe). Since the liquid stagnates at the V-section before the slugging, the liquid velocity V_L in Eq. (5) is assumed to be 0. The relation between V_G^2 and h_G for $D = 20$ mm and $\theta = 0^\circ$ ($V_G^2 = 1.90h_G$) is compared with experimental

data in Fig. 7 to examine the applicability of Eq. (5) to the prediction of the slug initiation. The measured data show almost linear relationships between V_G^2 and h_G . However, the profile does not pass through the origin and is steeper than Eq. (5). In the range of $h_G > 6$ mm (i.e., for low Q_L), the onset of slugging occurs at higher J_G than Eq. (5). This is because the liquid supply for the growth of the wave is small in the present configuration in which the liquid region is confined in the short length along the pipe, whereas the liquid has an unlimited length and the wave is able to grow along the pipe in the Mishima-Ishii's model. On the other hand, the measured J_G is lower than Eq. (5) at low h_G (i.e., for high Q_L). In this case, the gas flow passage area is extremely small due to the meniscus effect and the gas velocity becomes large even with low J_G . This causes the pressure reduction above the stagnant liquid, leading to the generation of liquid slug. As mentioned above, the present data are not explained by the Mishima-Ishii's model because of (i) the insufficient length of liquid region for the wave growth and (ii) the effect of the pressure reduction due to the increase in the gas velocity at the center of the V-section.

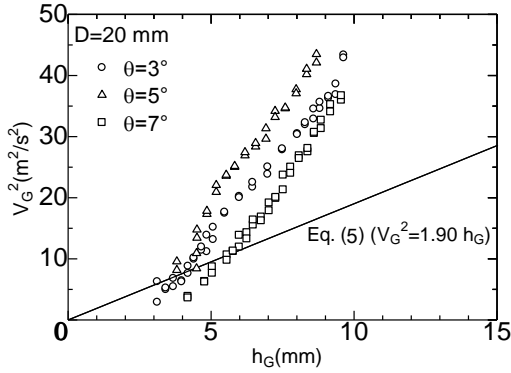


Figure 7: Comparison of measured onset of slugging with Mishima-Ishii's model

Since the inclination angle θ is small, the potential head can be ignored. Then the pressure drop ΔP at the V-section is represented by Bernoulli's law:

$$\Delta P = \frac{\rho_G}{2} (V_G^2 - J_G^2) \quad (6)$$

Considering that the slugging starts when the liquid head due to ΔP given by Eq. (6) becomes h_G , the onset of slugging can be expressed by

$$\Delta P = \frac{\rho_G}{2} (V_G^2 - J_G^2) = \rho_L g h_G \quad (7)$$

The measured data are plotted in terms of ΔP and h_G in Fig. 8. At high h_G , the experimental data for $\theta = 3^\circ$ and 5° are close to the line passing through the origin. However, they are approximately 20% of $\rho_L g h_G$ and their trend changes at $h_G \cong 5$ mm. In addition, the relation between ΔP and θ is not monotonous (i.e., ΔP becomes maximum at the intermediate inclination angle ($\theta = 5^\circ$)). These facts mean that the liquid head expressed by Eq. (7) is not the main cause of slug generation.

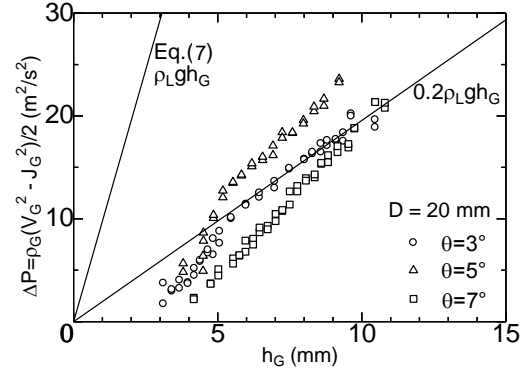


Figure 8: Relationship between ΔP and h_G

According to observation, the slugging is likely to start due to an instability of gas-liquid interface caused by the interfacial drag force. This is similar to flooding. The flooding has been modelled in terms of the Wallis parameter (Wallis, 1969; Whalley, 1987):

$$\sqrt{J_G^*} = \sqrt{\frac{\sqrt{\rho_G J_G}}{\sqrt{(\rho_L - \rho_G) g D}}} \quad (8)$$

The relation between $J_G^{*1/2}$ and Q_L^* ($Q_L^* = Q_L/Q_{Lmax}$, where Q_{Lmax} is the liquid volume which fills the whole area of the gas flow channel at the center of the V-section) is shown in Fig. 9. $J_G^{*1/2}$ linearly decreases with increasing Q_L^* and the effects of θ is small. The slugging can be, therefore, attributed to the interfacial shear force like flooding.

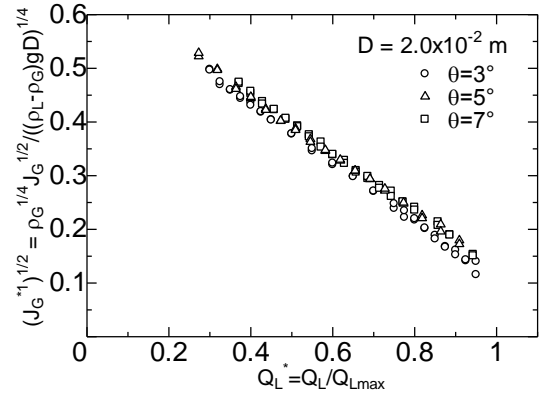


Figure 9: Relationship between $J_G^{*1/2}$ and Q_L^*

Empirical correlation for onset of slugging based on Wallis parameter

The effects of the parameters such as the inclination angle θ , pipe diameter D and fluid properties on the slugging are investigated, and an empirical correlation taking these parameters into account is presented.

The axial component of gravitational force, $g \sin \theta$, which pull the liquid back to the V-section, may contribute to stabilization of the liquid. The optimum form for representing the gravity effect is found to be:

$$\sqrt{J_G^{*2}} = \sqrt{\frac{\sqrt{\rho_G J_G}}{\sqrt{(\rho_L - \rho_G) g D (1 + \sin \theta)^4}}} \quad (9)$$

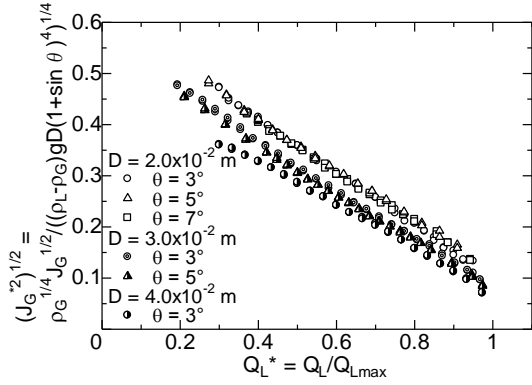


Figure 10: Effect of D on onset of slugging

Figure 10 shows the measured data for three pipe diameters in terms of $J_G^{*2/2}$ and Q_L^* . The dependence of D is significant especially at low Q_L^* because the shape of the interface is influenced by the meniscus effect. Thus the effect of surface tension is incorporated into the Wallis parameter by using the Bond number. Consequently the following expression for the modified Wallis parameter J_G^* is obtained.

$$\sqrt{J_G^*} = \bar{C} \sqrt{\frac{J_G}{f_g D}} \quad (10)$$

where

$$f_g = (1 + \sin \theta)^4 \frac{\rho_L - \rho_G}{\rho_G} g \quad (11)$$

and

$$\bar{C} = 1.73 \times 10^{-3} Bo + 0.912 \quad (12)$$

As shown in Fig. 11, the effect of liquid viscosity is small though the viscosity of the glycerol-water solution (40%) is 2.5 times as large as water. All the experimental data shown in Fig. 11 are well correlated with $J_G^{*1/2}$ and Q_L^* , i.e., the following empirical correlation can be recommended for the prediction of slugging:

$$\sqrt{J_G^*} = -0.52 Q_L^* + 0.62 \quad (13)$$

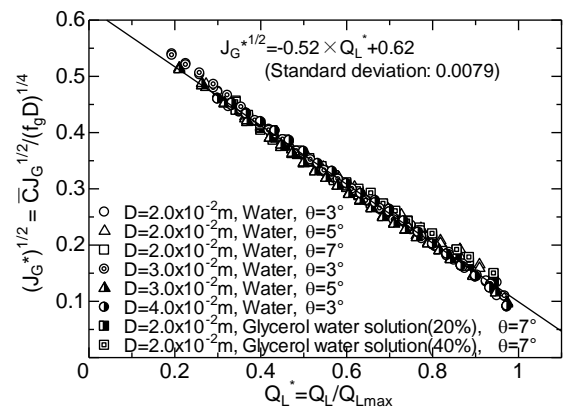


Figure 11: Relation between J_G^* and Q_L^*

Numerical prediction of onset of slugging

Figure 12 compares J_G at the onset of slugging obtained numerically and experimentally. The predicted J_G agree well with the measured data for all the pipe diameters. Figure 13 shows a comparison of different inclination angles for $D = 20$ mm. The prediction for small θ

underpredicts J_G especially at small Q_L , whereas the predictions for large θ agree well with the experiments. The reason is that the numerical simulation does not account for the surface tension. The meniscus effect on interface shape becomes significant at small θ for which the stagnant liquid widely spreads over gentle uphill and downhill of the pipe and the liquid is very thin near the periphery (see Fig. 2). Then the interface is no longer flat (i.e., shows convex shape) especially in the small pipe, while the interface in the simulation tends to be flat. At high Q_L , the numerical solution slightly overpredicts J_G (see Fig. 12) because the interface shape is affected by the surface tension and the gas flow area becomes extremely small. On the other hand, the discrepancies are small for the large pipe diameters $D = 40$ and 30 mm even with the small inclination angle ($\theta = 3^\circ$) as shown in Fig. 12. These results indicate that the effect of surface tension on the onset of slugging is relatively small for a large inclination angle or a large pipe diameter.

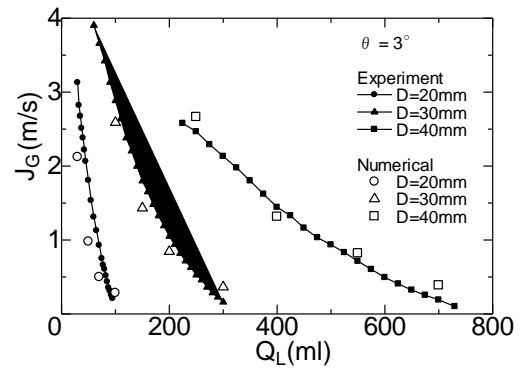


Figure 12: J_G at onset of slugging predicted by numerical simulation (effect of pipe diameter D)

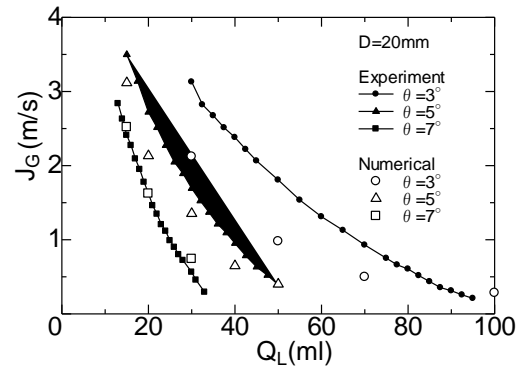


Figure 13: J_G at onset of slugging predicted by numerical simulation (effect of inclination angle θ)

The computed slugging (time-series cross-sectional profiles of a_L and liquid velocity) for the case of $D = 20$ mm, $\theta = 5^\circ$ and $Q_L = 40$ ml is shown in Fig. 14. Ripple grows to form a liquid slug (from 0 s to 0.8 s in Fig. 14) and the slug collapses and returns to the V-section due to the gravity to form another slug (from 0.8 s to 1.8 s in Fig. 14). This sequence agrees well with the observation.

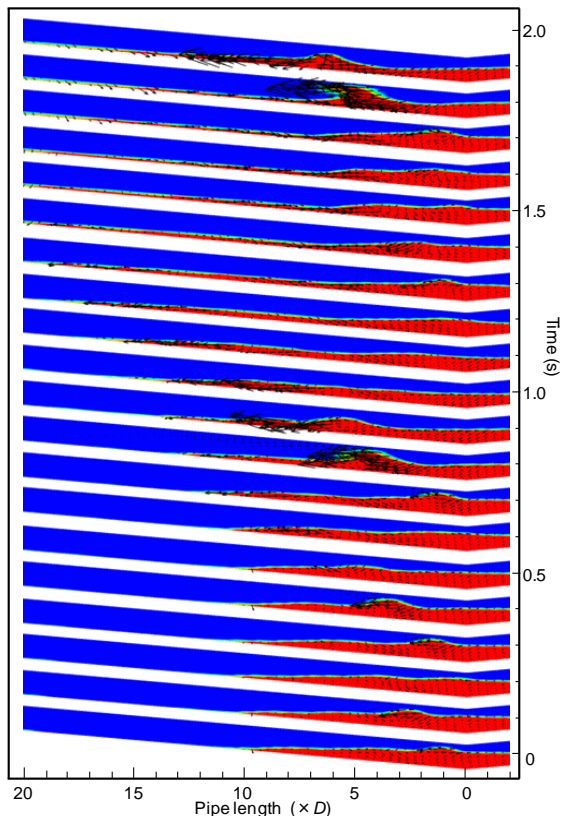


Figure 14: Time trace of computed slugging ($D = 20$ mm , $\theta = 5^\circ$ and $Q_L = 40$ ml)

CONCLUSION

Flow patterns and slugging of residual liquid at a V-shaped elbow were experimentally and numerically studied. The results are summarized as follows:

- (1) The flow pattern of residual liquid at the V-shaped elbow is classified into seven flow regimes, i.e. static puddle, wavy puddle, periodic slug flow, periodic semi-slug flow, aperiodic semi-slug flow, film flow and pebble flow.
- (2) The onset of slugging is well correlated in terms of the Wallis parameter, which has been utilized for modelling flooding phenomena in a pipe.
- (3) An empirical correlation based on a modified Wallis parameter, which accounts for the effects of inclination angle, pipe diameter and fluid properties, is proposed to predict the onset of slugging.
- (4) The two-fluid model is able to predict the onset of slugging with reasonable accuracy.

REFERENCES

- Kordyban, E.S., and Ranov, T., (1970), "Mechanism of slug formation in horizontal two-phase flow", *ASME. Journal of Basic Engineering*, Vol. 92, pp. 857-864.
- Wallis, G.B., and Dobson, J.E., (1973), "The onset of slugging in horizontal stratified air-water flow", *International Journal of Multiphase Flow*, Vol. 1, pp. 173-193.
- Mishima, K., and Ishii, M., (1980), "Theoretical prediction of onset of horizontal slug flow", *ASME. Journal of Fluids Engineering*, Vol. 102, pp. 441-445.

Mishima, K., and Ishii, M., (1993), "Measurement and analysis of slug characteristics in multiphase pipelines", *6th International Conference on Multiphase Production*, Cannes. *Mechanical Engineering Publications*, pp. 179-192.

Hosokawa, S., and Tomiyama, A., (2003), "Characteristics of liquid slug generated at a V-shaped elbow between inclined pipes", *The Japan Society of Mechanical Engineers, B*, Vol. 69, 686.

Zheng, G., Brill, J.P., and Shoham, O., (1993), "Slug flow behavior in a hilly terrain pipeline", *Society of Petroleum Engineers, Inc.*, pp. 529-541.

Masella, J.M., Tran, Q.H., Ferre, D., and Pauchon, C., (1998), "Transient simulation of two-phase flows in pipes", *International Journal of Multiphase Flow*, Vol. 24, pp. 739-755.

Issa, R.I., and Kempf, M.H.W., (2003), "Simulation of slug flow in horizontal and nearly horizontal pipes with the two-fluid model", *International Journal of Multiphase Flow*, Vol. 29, pp. 69-95.

Bonizzi, M., and Issa, R.I., (2003), "On the simulation of three-phase slug flow in nearly horizontal pipes using the multi-fluid model", *International Journal of Multiphase Flow*, Vol. 29, pp. 1719-1747.

Fitremann, J.M., (1975), "Methods for calculating two-phase flow in pipes", *International Journal of Multiphase Flow*, Vol. 3, pp. 117-122.

Wallis, G.B., (1969), *One-dimensional Two-phase Flow*, McGraw Hill, New York.

Whalley, P.B., (1987), *Boiling, Condensation and Gas-Liquid Flow*, Oxford Science Publications, New York.